PHYSICAL REVIEW D **85,** 091106(R) (2012)

Measurements of branching fractions and time-dependent *CP* violating asymmetries in $B^0 \to D^{(*)\pm} D^{\mp}$ decays

M. Röhrken,[18] I. Adachi,[8] H. Aihara,[51] D. M. Asner,[39] V. Aulchenko,[2] T. Aushev,[15] A. M. Bakich,[45] M. Barrett,[7] K. Belous,[14] V. Bhardwaj,[30] B. Bhuyan,[10] M. Bischofberger,[30] A. Bondar,[2] G. Bonvicini,[56] A. Bozek,[34] M. Bračko,[25,16] O. Brovchenko,[18] T. E. Browder,[7] M.-C. Chang,[5] A. Chen,[31] P. Chen,[33] B. G. Cheon,[6] K. Chilikin,[15] I.-S. Cho,[58] K. Cho,[19] Y. Choi,[44] J. Dalseno,[26,47] Z. Doležal,[3] Z. Drásal,[3] A. Drutskoy,[15] S. Eidelman,[2] J. E. Fast,[39] M. Feindt,[18] V. Gaur,[46] N. Gabyshev,[2] A. Garmash,[2] Y. M. Goh,[6] J. Haba,[8] H. Hayashii,[30] Y. Horii,[29] Y. Hoshi,[49] W.-S. Hou,[33] Y. B. Hsiung,[33] H. J. Hyun,[21] T. Iijima,[29,28] A. Ishikawa,[50] R. Itoh,[8] M. Iwabuchi,[58] Y. Iwasaki,[8] T. Julius,[27] J. H. Kang,[58] T. Kawasaki,[36] C. Kiesling,[26] H. J. Kim,[21] H. O. Kim,[21] J. B. Kim,[20] J. H. Kim,[19] K. T. Kim,[20] M. J. Kim,[21] Y. J. Kim,[19] K. Kinoshita,[4] B. R. Ko,[20] S. Koblitz,[26] P. Kodyš,[3] S. Korpar,[25,16] R. T. Kouzes,[39] P. Križan,[23,16] P. Krokovny,[2] B. Kronenbitter,[18] T. Kuhr,[18] T. Kumita,[53] Y.-J. Kwon,[58] S.-H. Lee,[20] J. Li,[43] Y. Li,[55] J. Libby,[11] C. Liu,[42] Y. Liu,[4] Z. Q. Liu,[12] D. Liventsev,[15] R. Louvot,[22] K. Miyabayashi,[30] H. Miyata,[36] R. Mizuk,[15] G. B. Mohanty,[46] A. Moll,[26,47] T. Mori,[28] N. Muramatsu,[41] Y. Nagasaka,[9] E. Nakano,[38] M. Nakao,[8] Z. Natkaniec,[34] S. Nishida,[8] O. Nitoh,[54] S. Ogawa,[48] T. Ohshima,[28] S. Okuno,[17] S. L. Olsen,[43,7] H. Ozaki,[8] G. Pakhlova,[15] C. W. Park,[44] H. Park,[21] H. K. Park,[21] K. S. Park,[44] T. K. Pedlar,[24] R. Pestotnik,[16] M. Petrič,[16] L. E. Piilonen,[55] A. Poluektov,[2] M. Prim,[18] K. Prothmann,[26,47] M. Ritter,[26] S. Ryu,[43] H. Sahoo,[7] Y. Sakai,[8] T. Sanuki,[50] Y. Sato,[50] O. Schneider,[22] C. Schwanda,[13] A. J. Schwartz,[4] K. Senyo,[57] O. Seon,[28] M. E. Sevior,[27] M. Shapkin,[14] C. P. Shen,[28] T.-A. Shibata,[52] J.-G. Shiu,[33] B. Shwartz,[2] A. Sibidanov,[45] F. Simon,[26,47] J. B. Singh,[40] P. Smerkol,[16] Y.-S. Sohn,[58] A. Sokolov,[14] E. Solovieva,[15] S. Stanič,[37] M. Starič,[16] K. Sumisawa,[8] T. Sumiyoshi,[53] K. Trabelsi,[8] M. Uchida,[52] S. Uehara,[8] Y. Unno,[6] S. Uno,[8] P. Urquijo,[1] P. Vanhoefer,[26] G. Varner,[7] K. E. Varvell,[45] V. Vorobyev,[2] C. H. Wang,[32] M.-Z. Wang,[33] P. Wang,[12] M. Watanabe,[36] Y. Watanabe,[17] K. M. Williams,[55] E. Won,[20] H. Yamamoto,[50] Y. Yamashita,[35] D. Zander,[18] Z. P. Zhang,[42] V. Zhilich,[2] V. Zhulanov,[2] and A. Zupanc[18]

(Belle Collaboration)

[1]*University of Bonn, Bonn*
[2]*Budker Institute of Nuclear Physics SB RAS and Novosibirsk State University, Novosibirsk 630090*
[3]*Faculty of Mathematics and Physics, Charles University, Prague*
[4]*University of Cincinnati, Cincinnati, Ohio 45221*
[5]*Department of Physics, Fu Jen Catholic University, Taipei*
[6]*Hanyang University, Seoul*
[7]*University of Hawaii, Honolulu, Hawaii 96822*
[8]*High Energy Accelerator Research Organization (KEK), Tsukuba*
[9]*Hiroshima Institute of Technology, Hiroshima*
[10]*Indian Institute of Technology Guwahati, Guwahati*
[11]*Indian Institute of Technology Madras, Madras*
[12]*Institute of High Energy Physics, Chinese Academy of Sciences, Beijing*
[13]*Institute of High Energy Physics, Vienna*
[14]*Institute of High Energy Physics, Protvino*
[15]*Institute for Theoretical and Experimental Physics, Moscow*
[16]*J. Stefan Institute, Ljubljana*
[17]*Kanagawa University, Yokohama*
[18]*Institut für Experimentelle Kernphysik, Karlsruher Institut für Technologie, Karlsruhe*
[19]*Korea Institute of Science and Technology Information, Daejeon*
[20]*Korea University, Seoul*
[21]*Kyungpook National University, Taegu*
[22]*École Polytechnique Fédérale de Lausanne (EPFL), Lausanne*
[23]*Faculty of Mathematics and Physics, University of Ljubljana, Ljubljana*
[24]*Luther College, Decorah, Iowa 52101*
[25]*University of Maribor, Maribor*
[26]*Max-Planck-Institut für Physik, München*
[27]*University of Melbourne, School of Physics, Victoria 3010*
[28]*Graduate School of Science, Nagoya University, Nagoya*
[29]*Kobayashi-Maskawa Institute, Nagoya University, Nagoya*
[30]*Nara Women's University, Nara*
[31]*National Central University, Chung-li*

[32]*National United University, Miao Li*
[33]*Department of Physics, National Taiwan University, Taipei*
[34]*H. Niewodniczanski Institute of Nuclear Physics, Krakow*
[35]*Nippon Dental University, Niigata*
[36]*Niigata University, Niigata*
[37]*University of Nova Gorica, Nova Gorica*
[38]*Osaka City University, Osaka*
[39]*Pacific Northwest National Laboratory, Richland, Washington 99352*
[40]*Panjab University, Chandigarh*
[41]*Research Center for Nuclear Physics, Osaka University, Osaka*
[42]*University of Science and Technology of China, Hefei*
[43]*Seoul National University, Seoul*
[44]*Sungkyunkwan University, Suwon*
[45]*School of Physics, University of Sydney, NSW 2006*
[46]*Tata Institute of Fundamental Research, Mumbai*
[47]*Excellence Cluster Universe, Technische Universität München, Garching*
[48]*Toho University, Funabashi*
[49]*Tohoku Gakuin University, Tagajo*
[50]*Tohoku University, Sendai*
[51]*Department of Physics, University of Tokyo, Tokyo*
[52]*Tokyo Institute of Technology, Tokyo*
[53]*Tokyo Metropolitan University, Tokyo*
[54]*Tokyo University of Agriculture and Technology, Tokyo*
[55]*CNP, Virginia Polytechnic Institute and State University, Blacksburg, Virginia 24061*
[56]*Wayne State University, Detroit, Michigan 48202*
[57]*Yamagata University, Yamagata*
[58]*Yonsei University, Seoul*

(Received 29 March 2012; published 18 May 2012)

We report measurements of branching fractions and time-dependent CP asymmetries in $B^0 \to D^+D^-$ and $B^0 \to D^{*\pm}D^{\mp}$ decays using a data sample that contains $(772 \pm 11) \times 10^6 B\bar{B}$ pairs collected at the $\Upsilon(4S)$ resonance with the Belle detector at the KEKB asymmetric-energy e^+e^- collider. We determine the branching fractions to be $\mathcal{B}(B^0 \to D^+D^-) = (2.12 \pm 0.16 \pm 0.18) \times 10^{-4}$ and $\mathcal{B}(B^0 \to D^{*\pm}D^{\mp}) = (6.14 \pm 0.29 \pm 0.50) \times 10^{-4}$. We measure CP asymmetry parameters $\mathcal{S}_{D^+D^-} = -1.06^{+0.21}_{-0.14} \pm 0.08$ and $\mathcal{C}_{D^+D^-} = -0.43 \pm 0.16 \pm 0.05$ in $B^0 \to D^+D^-$ and $\mathcal{A}_{D^*D} = +0.06 \pm 0.05 \pm 0.02$, $\mathcal{S}_{D^*D} = -0.78 \pm 0.15 \pm 0.05$, $\mathcal{C}_{D^*D} = -0.01 \pm 0.11 \pm 0.04$, $\Delta\mathcal{S}_{D^*D} = -0.13 \pm 0.15 \pm 0.04$ and $\Delta\mathcal{C}_{D^*D} = +0.12 \pm 0.11 \pm 0.03$ in $B^0 \to D^{*\pm}D^{\mp}$, where the first uncertainty is statistical and the second is systematic. We exclude the conservation of CP symmetry in both decays at equal to or greater than 4σ significance.

DOI: 10.1103/PhysRevD.85.091106 PACS numbers: 13.25.Hw, 11.30.Er, 12.15.Ff

In the standard model (SM) of electroweak interactions, the effect of CP violation is explained by a single complex phase in the three-family Cabibbo-Kobayashi-Maskawa quark-mixing matrix [1]. Both the Belle and *BABAR* Collaborations experimentally established this effect [2,3] and precisely determined the parameter $\sin 2\phi_1$ by measurements of mixing-induced CP asymmetries in $b \to (c\bar{c})s$ transitions, where $\phi_1 = \arg[-V_{cd}V_{cb}^*/V_{td}V_{tb}^*]$ [4–6].

In $b \to c\bar{c}d$ transitions such as $B^0 \to D^{(*)\pm}D^{\mp}$ decays, the dominant contributions are Cabibbo-disfavored but color-allowed tree-level diagrams and the corresponding mixing-induced CP asymmetries are directly related to $\sin 2\phi_1$. In addition, $b \to d$ penguin diagrams that may have different weak phases can contribute to these decays. Theoretical considerations based on models using factorization approximations and heavy quark symmetry predict the corrections to mixing-induced CP violation to be a few percent and possible direct CP violation to be negligibly small [7].

CP violation in $b \to c\bar{c}d$ transitions has been studied previously by the Belle and *BABAR* Collaborations. In $B^0 \to D^+D^-$ decays using a data sample of $535 \times 10^6 B\bar{B}$ pairs, Belle found evidence of a large direct CP violation: $\mathcal{C}_{D^+D^-} = -0.91 \pm 0.23 \pm 0.06$ corresponding to a 3.2σ deviation from zero [8,9], in contradiction to theoretical expectations [7]. This deviation was not confirmed by *BABAR* and has not been observed in other $B^0 \to D^{*\pm}D^{(*)\mp}$ decay modes [10–12].

In this article we present measurements of branching fractions and CP violating asymmetries in the decays $B^0 \to D^+D^-$ and $B^0 \to D^{*\pm}D^{\mp}$ using the final data sample of the Belle experiment.

The decay rate of a neutral B meson decaying to a CP eigenstate such as D^+D^- is given by

$$f_{D^+D^-}(\Delta t) = \frac{e^{-|\Delta t|/\tau_{B^0}}}{4\tau_{B^0}}\{1 + q[\mathcal{S}_{D^+D^-}\sin(\Delta m_d \Delta t) - \mathcal{C}_{D^+D^-}\cos(\Delta m_d \Delta t)]\}, \quad (1)$$

where $q = +1(-1)$ represents the b-flavor charge when the accompanying B meson is tagged as a $B^0(\bar{B}^0)$, and Δt represents the proper time interval between the two neutral B decays in an $\Upsilon(4S)$ event. The B^0 lifetime is denoted by τ_{B^0} and the mass difference between the two neutral B mass eigenstates by Δm_d. The parameters $\mathcal{S}_{D^+D^-}$ and $\mathcal{C}_{D^+D^-}$ measure mixing-induced and direct CP violation, respectively [9].

Unlike D^+D^-, $D^{*+}D^-$ and $D^{*-}D^+$ are not CP eigenstates. The decay rate of neutral B mesons decaying to these states has four flavor-charge configurations and can be expressed as [13,14]

$$f_{D^{*\pm}D^{\mp}}(\Delta t) = (1 \pm \mathcal{A}_{D^*D})\frac{e^{-|\Delta t|/\tau_{B^0}}}{8\tau_{B^0}} \times \{1 + q[(\mathcal{S}_{D^*D} \pm \Delta\mathcal{S}_{D^*D})\sin(\Delta m_d \Delta t) - (\mathcal{C}_{D^*D} \pm \Delta\mathcal{C}_{D^*D})\cos(\Delta m_d \Delta t)]\}, \quad (2)$$

where the $+$ $(-)$ sign represents the $D^{*+}D^-$ $(D^{*-}D^+)$ final state. The time- and flavor-integrated charge asymmetry $\mathcal{A}_{D^*D}$ measures direct CP violation. The quantity $\mathcal{S}_{D^*D}$ parameterizes mixing-induced CP violation and $\mathcal{C}_{D^*D}$ parameterizes flavor-dependent direct CP violation. The quantities $\Delta\mathcal{C}_{D^*D}$ and $\Delta\mathcal{S}_{D^*D}$ are not sensitive to CP violation. The parameter $\Delta\mathcal{C}_{D^*D}$ describes the asymmetry between the rates $\Gamma(B^0 \to D^{*-}D^+) + \Gamma(\bar{B}^0 \to D^{*+}D^-)$ and $\Gamma(B^0 \to D^{*+}D^-) + \Gamma(\bar{B}^0 \to D^{*-}D^+)$. The parameter $\Delta\mathcal{S}_{D^*D}$ is related to the relative strong phase between the amplitudes contributing to the decays.

This analysis is based on a data sample containing $(772 \pm 11) \times 10^6 B\bar{B}$ pairs collected at the $\Upsilon(4S)$ resonance with the Belle detector at the KEKB asymmetric-energy e^+e^- collider [15]. The $\Upsilon(4S)$ is produced with a Lorentz boost of $\beta\gamma = 0.425$ close to an axis along the e^- beam, which allows the determination of Δt from the displacement of decay vertices of both B mesons.

The Belle detector is a large-solid-angle magnetic spectrometer that is described in detail in Ref. [16]. The present analysis uses for track reconstruction and particle identification a silicon vertex detector (SVD), a 50-layer central drift chamber (CDC), an array of aerogel threshold Cherenkov counters (ACC), a barrel-like arrangement of time-of-flight scintillation counters (TOF), and an electromagnetic calorimeter (ECL) composed of CsI(Tl) crystals located inside a superconducting solenoid coil that provides a 1.5 T magnetic field.

Reconstructed charged tracks are required to have a transverse (longitudinal) distance of closest approach to the interaction point (IP) of less than 2 (4) cm. For identification of charged particles (PID), measurements of specific energy loss in the CDC and measurements from the ACC and TOF are combined in a likelihood-ratio approach. The selection requirement on the combined PID quantity has a kaon (pion) identification efficiency of 91% (99%) with an associated pion (kaon) misidentification rate of 2% (18%). Charged tracks are also required to be not positively identified as electrons by measurements of shower shapes and energy deposited in the ECL. Neutral pions are reconstructed from two photons detected in the ECL with each photon having an energy greater than 30 MeV. The invariant mass of the photon pair is required to be within 15 MeV/c^2 of the nominal π^0 mass (corresponding to a width of 3.3σ). For π^0 candidates a kinematic fit to the IP profile with a mass constraint is performed. Neutral kaons are reconstructed in the decay mode $K^0_S \to \pi^+\pi^-$. The invariant mass of the $\pi^+\pi^-$ pair is required to be within 15 MeV/c^2 of the nominal K^0_S mass (5.8σ). Additional momentum-dependent selection requirements consider the possible displacement of the K^0_S decay vertices from the IP [17].

Charged D mesons are reconstructed in the decay modes $D^+ \to K^-\pi^+\pi^+$ and $D^+ \to K^0_S\pi^+$ [18]. The invariant mass of D^+ candidates is required to be within 12 MeV/c^2 of the nominal mass (3.4σ in $D^+ \to K^-\pi^+\pi^+$ and 2.9σ in $D^+ \to K^0_S\pi^+$). Neutral D mesons are reconstructed in the decay modes $D^0 \to K^-\pi^+$, $D^0 \to K^-\pi^+\pi^+\pi^-$, $K^0_S\pi^+\pi^-$, and $D^0 \to K^-\pi^+\pi^0$. The invariant mass of D^0 candidates is required to be within 15 MeV/c^2 (3.3σ–3.7σ) of the nominal mass, except for the $D^0 \to K^-\pi^+\pi^0$ decay mode where a requirement of 32 MeV/c^2 (3.0σ) is applied. We reconstruct D^{*+} mesons in the decay modes $D^{*+} \to D^0\pi^+$ and $D^{*+} \to D^+\pi^0$. The momentum resolution of charged low momentum pions from D^{*+} decays, referred to as soft pions, is improved by a kinematic fit in which the soft pion is constrained to the D^{*+} decay vertex determined from a kinematic fit of D candidates constrained to originate from the IP profile. The difference of invariant masses of the D^{*+} and $D^0(D^+)$ candidates is required to be within 1.5 MeV/c^2 (2.5 MeV/c^2) (3.1σ–3.7σ) of the nominal mass difference, except for modes involving $D^0 \to K^-\pi^+\pi^+\pi^-$ and $D^0 \to K^-\pi^+\pi^0$ decays where a requirement of 2 MeV/c^2 (4.6σ and 3.2σ) is applied.

Neutral B mesons are reconstructed by combining $D^{(*)+}$ and D^- candidates, and selected by the beam-energy-constrained mass $M_{\rm bc} = \sqrt{(E^*_{\rm beam}/c^2)^2 - (p^*_B/c)^2}$ and the energy difference $\Delta E = E^*_B - E^*_{\rm beam}$, where $E^*_{\rm beam}$ is the energy of the beam and p^*_B and E^*_B are the momentum and energy of the B^0 candidates in the center-of-mass frame. The selected regions are $5.2\ {\rm GeV}/c^2 < M_{\rm bc} < 5.3\ {\rm GeV}/c^2$ and $-50\ {\rm MeV} < \Delta E < 100\ {\rm MeV}$. The lower boundary in ΔE was chosen to exclude reflections from misidentified $B^0 \to D^+_s D^{(*)-}$ decays that populate the $M_{\rm bc}$ signal region at $\Delta E \approx -75$ MeV.

In $B^0 \to D^+D^-(B^0 \to D^{*\pm}D^{\mp})$, after applying the above selection requirements, 12% (16%) of the signal

events contain more than one B^0 candidate. In this case the candidate with the smallest quadratic sum of deviations of reconstructed invariant masses of D daughters (and mass differences of D^{*+} daughters) from nominal values, divided by the width of corresponding signal peaks, is selected. This requirement selects the correct candidate with a probability of 96% (92%).

In $B^0 \to D^+D^-$ unlike in $B^0 \to D^{*\pm}D^{\mp}$ the major source of background arises from $e^+e^- \to q\bar{q}$ ($q \in \{u, d, s, c\}$) continuum events. This background is suppressed by a neural network (NN) implemented by the NeuroBayes package [19] that combines information about the event topology. Observables included in the NN are $\cos\theta_B^*$, where θ_B^* is the polar angle of the B^0 candidate with respect to the beam direction in the center-of-mass frame, a combination of 16 modified Fox-Wolfram moments [20], and the momentum flow in nine concentric cones around the thrust axis of the B^0 candidate [21]. The requirement on the NN selection rejects 64% of the background while retaining 92% of the signal.

The signal yields are obtained by two-dimensional unbinned extended maximum likelihood fits to the $M_{\rm bc}$ and ΔE distributions. The $M_{\rm bc}$ distributions are parameterized by a Gaussian function for the signal component and by an empirically determined threshold function introduced by the ARGUS Collaboration [22] for the background component. The ΔE distributions are parameterized by the sum of two Gaussian functions (the sum of a Gaussian function and an empirically determined function introduced by the Crystal Ball Collaboration [23]) with common mean for the signal component in $B^0 \to D^+D^-(B^0 \to D^{*\pm}D^{\mp})$ and by a linear function for the background component. The shape parameters of signal components in $B^0 \to D^+D^-(B^0 \to D^{*\pm}D^{\mp})$ are fixed to values obtained from $B^0 \to D_s^+D^-(B^0 \to D_s^+D^{*-})$ data distributions, where the relative widths and fractions of the signal components in ΔE are fixed to values obtained from Monte Carlo (MC) simulation studies. The $M_{\rm bc}$ and ΔE distributions and fit projections are shown in Fig. 1. For $B^0 \to D^+D^-$ the obtained yields are 221.4 ± 18.6 signal events in the $(K^-\pi^+\pi^+)(K^+\pi^-\pi^-)$ final state and 48.0 ± 8.9 signal events in the $(K^-\pi^+\pi^+)(K_S^0\pi^-)$ final state.

For $B^0 \to D^{*\pm}D^{\mp}$, we obtain a yield of 886.8 ± 39.3 signal events in all reconstructed modes combined. Of these, the yield in modes involving $D^{*+} \to D^0\pi^+$ decays only is 769.2 ± 36.0 signal events.

Decays such as $B^0 \to D^{(*)-}K^{*+}$, $B^0 \to D^{(*)-}K^0\pi^+$, and $B^0 \to D^{(*)-}\pi^+\pi^+\pi^-$ have the same final states as the reconstructed $B^0 \to D^+D^{(*)-}$ decay modes and can possibly populate the $M_{\rm bc}$ and ΔE signal region. The contributions of such decays, referred to as peaking background, are estimated from D mass sidebands and subtracted in the signal yields given above. For $B^0 \to D^+D^-(B^0 \to D^{*\pm}D^{\mp})$, we find a contribution of $0.7 \pm 1.5(4.7 \pm 2.1)$ peaking background events from fits to $D^- \to K_S^0\pi^-$ mass sidebands. The $D^- \to K^+\pi^-\pi^-$ mass sidebands are considered to be free of peaking background and no background subtraction is performed. This assumption has been tested by MC simulations and no peaking background is found in the data sidebands.

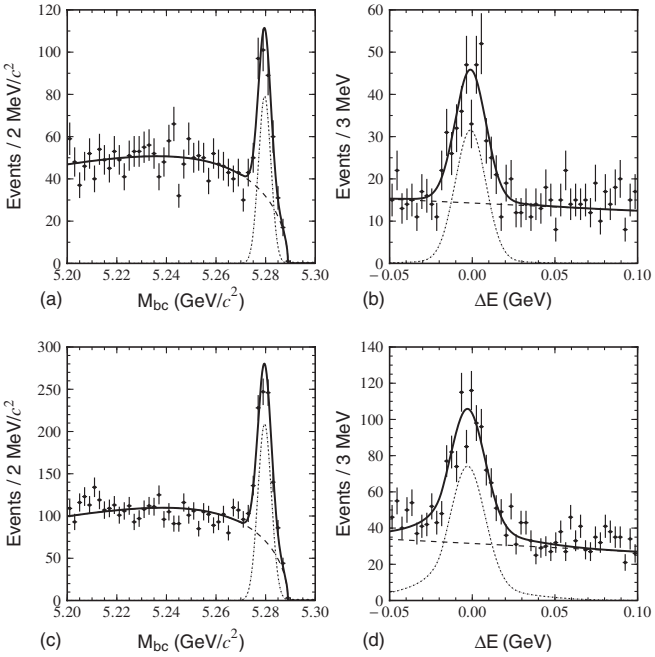

FIG. 1. $M_{\rm bc}$ and ΔE distributions (data points with error bars) and fit projections (solid lines) for (a)–(b) $B^0 \to D^+D^-$ and (c)–(d) $B^0 \to D^{*\pm}D^{\mp}$ decays. The dotted (dashed) lines represent projections of signal (background) fit components. A $|\Delta E| < 30$ MeV ($M_{\rm bc} > 5.27$ GeV/c^2) requirement is applied in plotting the $M_{\rm bc}(\Delta E)$ distributions.

The reconstruction efficiencies are obtained from MC simulations of signal decays and have been corrected to account for PID selection efficiency differences between MC simulations and data. To exclude systematic effects in the determination of reconstruction efficiencies associated with soft neutral pions, only modes involving $D^{*+} \to D^0\pi^+$ decays are used in the $B^0 \to D^{*\pm}D^{\mp}$ branching fraction measurement.

The branching fractions are calculated from signal yields, reconstruction efficiencies, the number of $B\bar{B}$ events, and current world averages of D^0, D^+, and D^{*+} branching fractions [24]. The branching fraction for $B^0 \to D^+D^-$ decays is calculated as the weighted average of the branching fractions determined for each of both reconstructed decay modes separately. The branching fraction for $B^0 \to D^{*\pm}D^{\mp}$ decays is determined by the signal yield in all modes and the average reconstruction efficiency weighted by the D branching fractions. The determined branching fractions are $\mathcal{B}(B^0 \to D^+D^-) = (2.12 \pm 0.16 \pm 0.18) \times 10^{-4}$ and $\mathcal{B}(B^0 \to D^{*\pm}D^{\mp}) = (6.14 \pm 0.29 \pm 0.50) \times 10^{-4}$. The systematic uncertainties of the measured branching fractions are summarized in Table I.

TABLE I. Summary of systematic uncertainties of the $B^0 \to D^+D^-$ and $B^0 \to D^{*\pm}D^{\mp}$ branching fractions (in %).

Source	D^+D^-	$D^{*\pm}D^{\mp}$
Track reconstruction efficiency	2.0	4.1
K^0_S reconstruction efficiency	0.7	0.7
π^0 reconstruction efficiency	-	1.6
K/π selection efficiency	5.5	5.3
Event reconstruction efficiency	1.0	0.1
Continuum suppression	4.1	-
Fit models	1.1	0.6
D branching fractions	4.3	3.9
Number of $B\bar{B}$ events	1.4	1.4
Total	8.6	8.1

The uncertainties due to track, K^0_S and π^0 reconstruction efficiency, and the uncertainty due to the K/π selection efficiency have been estimated using studies of D^{*+} decays with MC simulations and data. The effect on the event reconstruction efficiencies due to broader D mass distributions for data and the corresponding selection is studied by a MC/data comparison and assigned as a systematic uncertainty. As the systematic uncertainty of the applied continuum suppression in $B^0 \to D^+D^-$, the maximum variation of signal yields in a MC/data comparison of the neural networks using $B^0 \to D^+_s D^-$ decays is assigned. The contributions due to the fit models are estimated by varying the fixed parameters within their uncertainties. The contributions due to uncertainties of the D^0, D^+, and D^{*+} branching fractions and of the number of $B\bar{B}$ events are obtained by propagation of the appropriate uncertainties. The total systematic uncertainties are obtained by adding all contributions in quadrature.

The technique used to determine the CP asymmetry parameters from Δt distributions is described in detail in Ref. [5]. The decay vertex of the signal B meson is reconstructed from a kinematic fit of the two D mesons to a common vertex including information about the IP profile. No information about soft pions is used in the vertex reconstruction. The decay vertex and the flavor of the accompanying B meson is obtained by an inclusive approach using the remaining charged tracks that are not used in the signal B reconstruction. Requirements on the quality of reconstructed B vertices and on the number of hits in the silicon vertex detector are applied. The algorithms applied to obtain the b-flavor-charge q and a tagging quality variable r are described in detail in Ref. [25]. The variable r is related to the mistag fractions determined from $b \to c$ control samples and ranges from $r = 0$ (no flavor discrimination) to $r = 1$ (unambiguous flavor assignment). The data is divided into seven r intervals.

The CP asymmetry parameters are determined by unbinned maximum likelihood fits to the Δt distributions. The probability density function (PDF) used to describe the Δt distributions is given by

$$P = (1 - f_{\rm ol}) \sum_k f_k \int [\mathcal{P}_k(\Delta t') R_k(\Delta t - \Delta t')] d(\Delta t') + f_{\rm ol} P_{\rm ol}(\Delta t), \quad (3)$$

where the index k denotes signal and background components and the fraction f_k depends on the r interval and is evaluated on an event-by-event basis as a function of $M_{\rm bc}$ and ΔE. The signal component consists of the convolution of distributions given by modifications of Eqs. (1) and (2) that include the effect of incorrect flavor assignments and of a resolution function to account for the finite resolution of the vertex reconstruction [26]. The background component is parameterized by the convolution of the sum of a prompt and an exponential distribution allowing for effective lifetimes and a resolution function composed of the sum of two Gaussian functions. The parameters of the background components are fixed to values determined by fits to $M_{\rm bc} < 5.26\ {\rm GeV}/c^2$ sidebands. A Gaussian function $P_{\rm ol}$ with a broad width of about 35 ps and a small fraction $f_{\rm ol}$ of about 2×10^{-4} is added to account for outlier events with large Δt.

The free parameters in the $B^0 \to D^+D^-$ fit are $\mathcal{S}_{D^+D^-}$ and $\mathcal{C}_{D^+D^-}$ and the free parameters in the $B^0 \to D^{*\pm}D^{\mp}$ fit are $\mathcal{A}_{D^*D}$, $\mathcal{S}_{D^*D}$, $\mathcal{C}_{D^*D}$, $\Delta\mathcal{S}_{D^*D}$, and $\Delta\mathcal{C}_{D^*D}$. The lifetime τ_{B^0} and mass difference Δm_d are fixed to current world averages [24]. The fits are performed in a signal region defined by $|\Delta E| < 30$ MeV and $5.27\ {\rm GeV}/c^2 < M_{\rm bc} < 5.29\ {\rm GeV}/c^2$. The signal purity is 62% (59%) for $B^0 \to D^+D^-(B^0 \to D^{*\pm}D^{\mp})$. For $B^0 \to D^+D^-$ the results are

$$\begin{aligned} \mathcal{S}_{D^+D^-} &= -1.06^{+0.21}_{-0.14} \pm 0.08, \\ \mathcal{C}_{D^+D^-} &= -0.43 \pm 0.16 \pm 0.05, \end{aligned} \quad (4)$$

and for $B^0 \to D^{*\pm}D^{\mp}$

$$\begin{aligned} \mathcal{A}_{D^*D} &= +0.06 \pm 0.05 \pm 0.02, \\ \mathcal{S}_{D^*D} &= -0.78 \pm 0.15 \pm 0.05, \\ \mathcal{C}_{D^*D} &= -0.01 \pm 0.11 \pm 0.04, \\ \Delta\mathcal{S}_{D^*D} &= -0.13 \pm 0.15 \pm 0.04, \\ \Delta\mathcal{C}_{D^*D} &= +0.12 \pm 0.11 \pm 0.03, \end{aligned} \quad (5)$$

where the first uncertainty is statistical and the second systematic. The Δt distributions and projections of the fits are shown in Fig. 2.

The systematic uncertainties in the CP asymmetry parameters are evaluated for each decay mode and are summarized in Table II. Sources of systematic uncertainties on the vertex reconstruction are the IP profile constraint, requirements on the vertex fit quality for signal and tagging B mesons, and requirements on impact parameters of tracks in the reconstruction of the tagging B meson and the Δt fit range. These contributions are estimated by variations of each of the applied requirements. Further contributions to the vertex reconstruction are a global

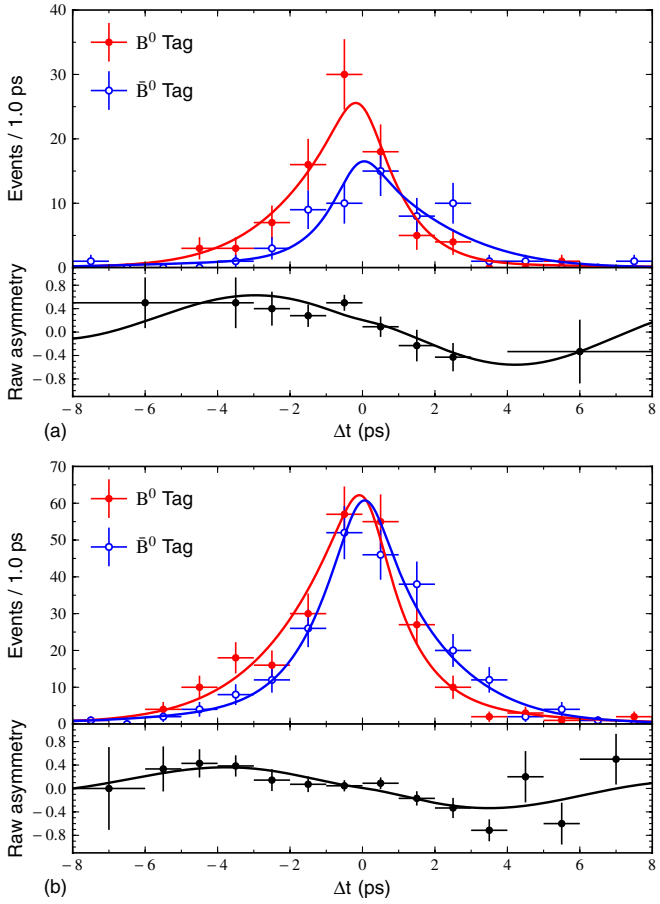

FIG. 2 (color online). Top: Δt distributions (data points with error bars) of (a) $B^0 \to D^+D^-$ and (b) $B^0 \to D^{*+}D^- + B^0 \to D^{*-}D^+$ candidates associated with high quality flavor tags ($r > 0.5$). The lines show projections of the sum of signal and background components in the fit. The signal purity for $r > 0.5$ is 69% (66%) for $B^0 \to D^+D^-(B^0 \to D^{*\pm}D^{\mp})$. Bottom: The CP asymmetry obtained from the above distributions and projections.

SVD misalignment and a Δz bias, which are both estimated by MC simulations. The contributions due to the Δt resolution functions, the Δt parameterization of background components, and the calculation of the signal purity and the physics parameters τ_{B^0} and Δm_d are estimated by varying the fixed parameters within their uncertainties. The systematic uncertainty due to flavor tagging is estimated by varying the mistag fractions in each r interval within their uncertainties. A possible fit bias is estimated from a large sample of MC simulated signal decays. The effect of the peaking background is studied using MC simulations allowing for CP violation in nonresonant decays. The possible interference between Cabibbo-favored $b \to c\bar{u}d$ and suppressed $\bar{b} \to \bar{u}c\bar{d}$ amplitudes in the decay of the tagging B meson, referred to as tag-side interference [27], is studied using MC simulations with inputs obtained from $B^0 \to D^{*-}\ell^+\nu_\ell$ control samples. The largest deviations in the above MC studies are assigned as systematic uncertainties. The total systematic uncertainty is obtained by adding all contributions in quadrature.

The significance of the results is studied by a likelihood-ratio approach. For $B^0 \to D^+D^-$ we exclude the conservation of CP symmetry ($\mathcal{S}_{D^+D^-} = \mathcal{C}_{D^+D^-} = 0$) at a confidence level of $1\text{–}2.7 \times 10^{-5}$ corresponding to 4.2σ. For $B^0 \to D^{*\pm}D^{\mp}$ the conservation of CP symmetry ($\mathcal{A}_{D^*D} = \mathcal{S}_{D^*D} = \mathcal{C}_{D^*D} = 0$) is excluded at a confidence level of $1\text{–}6.8 \times 10^{-5}$ corresponding to 4.0σ. These results account for both the statistical and the systematic uncertainties.

The fit procedure was validated by various cross-checks. The same analysis was performed for $B^0 \to D_s^+D^{(*)-}$ decays. The results are $\mathcal{A}_{D_sD} = -0.01 \pm 0.02$, $\mathcal{S}_{D_sD} = -0.05 \pm 0.05$, $\mathcal{C}_{D_sD} = +0.01 \pm 0.03$, $\Delta\mathcal{S}_{D_sD} = +0.01 \pm 0.05$, and $\Delta\mathcal{C}_{D_sD} = -0.95 \pm 0.03$ in $B^0 \to D_s^+D^-$ and $\mathcal{A}_{D_sD^*} = +0.01 \pm 0.02$, $\mathcal{S}_{D_sD^*} = -0.04 \pm 0.05$, $\mathcal{C}_{D_sD^*} = +0.06 \pm 0.03$, $\Delta\mathcal{S}_{D_sD^*} = +0.10 \pm 0.05$, and $\Delta\mathcal{C}_{D_sD^*} = -1.00 \pm 0.03$ in $B^0 \to D_s^+D^{*-}$, where the uncertainties are statistical only. The results are consistent with the assumption of no CP violation in $B^0 \to D_s^+D^{(*)-}$ decays. The lifetimes determined by fits to untagged $B^0 \to D^+D^-$ and $B^0 \to D^{*\pm}D^{\mp}$ samples are consistent with the world average [24].

In summary we report measurements of the branching fractions and time-dependent CP violating asymmetries in

TABLE II. Summary of systematic uncertainties in the time-dependent CP asymmetry parameters for $B^0 \to D^+D^-$ and $B^0 \to D^{*\pm}D^{\mp}$ decays (in units of 10^{-2}).

Source	$\mathcal{S}_{D^+D^-}$	$\mathcal{C}_{D^+D^-}$	$\mathcal{A}_{D^*D}$	$\mathcal{S}_{D^*D}$	$\mathcal{C}_{D^*D}$	$\Delta\mathcal{S}_{D^*D}$	$\Delta\mathcal{C}_{D^*D}$
Vertex reconstruction	3.6	2.2	1.3	2.5	2.3	2.4	2.3
Δt resolution function	6.5	2.4	0.4	3.5	1.1	1.9	0.6
Background Δt PDFs	2.7	0.5	0.2	0.7	0.2	0.5	0.1
Signal purity	1.2	1.8	0.2	0.9	0.4	0.3	0.2
Physics parameters	0.7	0.4	<0.1	0.2	0.1	0.2	<0.1
Flavor tagging	0.7	0.6	<0.1	0.4	0.3	0.3	0.2
Possible fit bias	0.8	0.2	0.6	0.8	1.1	0.8	0.5
Peaking background	0.3	0.9	0.4	1.3	0.5	0.8	0.7
Tag-side interference	1.4	3.2	0.2	1.1	3.1	0.9	0.6
Total	8.2	5.1	1.6	4.9	4.3	3.5	2.6

$B^0 \to D^+D^-$ and $B^0 \to D^{*\pm}D^{\mp}$ decays using the final Belle data sample of $(772 \pm 11) \times 10^6 B\bar{B}$ pairs. We measure the branching fractions $\mathcal{B}(B^0 \to D^+D^-) = (2.12 \pm 0.16 \pm 0.18) \times 10^{-4}$ and $\mathcal{B}(B^0 \to D^{*\pm}D^{\mp}) = (6.14 \pm 0.29 \pm 0.50) \times 10^{-4}$. The measured CP asymmetry parameters are $\mathcal{S}_{D^+D^-} = -1.06^{+0.21}_{-0.14} \pm 0.08$ and $\mathcal{C}_{D^+D^-} = -0.43 \pm 0.16 \pm 0.05$ in $B^0 \to D^+D^-$ and $\mathcal{A}_{D^*D} = +0.06 \pm 0.05 \pm 0.02$, $\mathcal{S}_{D^*D} = -0.78 \pm 0.15 \pm 0.05$, $\mathcal{C}_{D^*D} = -0.01 \pm 0.11 \pm 0.04$, $\Delta\mathcal{S}_{D^*D} = -0.13 \pm 0.15 \pm 0.04$, and $\Delta\mathcal{C}_{D^*D} = +0.12 \pm 0.11 \pm 0.03$ in $B^0 \to D^{*\pm}D^{\mp}$. For $B^0 \to D^+D^-$, the CP asymmetries are approximately 0.5σ outside of the physical parameter space defined by $\sqrt{\mathcal{S}^2_{D^+D^-} + \mathcal{C}^2_{D^+D^-}} \leq 1$ and the direct CP asymmetry deviates from zero by approximately 2.0σ. For $B^0 \to D^{*\pm}D^{\mp}$, if the contribution of penguin diagrams is negligible and if the hadronic phase between $B^0 \to D^{*+}D^-$ and $B^0 \to D^{*-}D^+$ amplitudes is zero and their magnitudes are the same, then $\mathcal{A}_{D^*D}$, $\mathcal{C}_{D^*D}$, $\Delta\mathcal{S}_{D^*D}$, and $\Delta\mathcal{C}_{D^*D}$ vanish and $\mathcal{S}_{D^*D}$ is equal to $\sin 2\phi_1$. Our result is consistent with the above and we measure $\sin 2\phi_1 = -0.78 \pm 0.15 \pm 0.05$. The CP asymmetries obtained in $B^0 \to D^+D^-$ and $B^0 \to D^{*\pm}D^{\mp}$ decays are both in agreement with measurements of decays involving $b \to (c\bar{c})s$ transitions [4,5] and with previous measurements of $B^0 \to D^{(*)\pm}D^{(*)\mp}$ decays [8,10–12]. We find evidence for CP violation in both decay channels with a significance of $\geq 4\sigma$. These results supersede previous measurements of branching fractions and time-dependent CP asymmetries in $B^0 \to D^+D^-$ and $B^0 \to D^{*\pm}D^{\mp}$ by the Belle Collaboration [8,10,28].

We thank the KEKB group for excellent operation of the accelerator; the KEK cryogenics group for efficient solenoid operations; and the KEK computer group, the NII, and PNNL/EMSL for valuable computing and SINET4 network support. We acknowledge support from MEXT, JSPS and Nagoya's TLPRC (Japan); ARC and DIISR (Australia); NSFC (China); MSMT (Czechia); DST (India); INFN (Italy); MEST, NRF, GSDC of KISTI, and WCU (Korea); MNiSW (Poland); MES and RFAAE (Russia); ARRS (Slovenia); SNSF (Switzerland); NSC and MOE (Taiwan); and DOE and NSF (USA).

[1] N. Cabibbo, Phys. Rev. Lett. **10**, 531 (1963); M. Kobayashi and T. Maskawa, Prog. Theor. Phys. **49**, 652 (1973).
[2] K. Abe *et al.* (Belle Collaboration), Phys. Rev. Lett. **87**, 091802 (2001).
[3] B. Aubert *et al.* (*BABAR* Collaboration), Phys. Rev. Lett. **87**, 091801 (2001).
[4] B. Aubert *et al.* (*BABAR* Collaboration), Phys. Rev. D **79**, 072009 (2009).
[5] I. Adachi *et al.* (Belle Collaboration), Phys. Rev. Lett. **108**, 171802 (2012).
[6] Another naming convention, $\beta(=\phi_1)$, is also used in the literature.
[7] Z. Z. Xing, Phys. Lett. B **443**, 365 (1998); Z. Z. Xing, Phys. Rev. D **61**, 014010 (1999).
[8] S. Fratina *et al.* (Belle Collaboration), Phys. Rev. Lett. **98**, 221802 (2007).
[9] Another naming convention for direct CP asymmetries, $\mathcal{A}(=-\mathcal{C})$, in decays to CP eigenstates is used in Ref. [8] and in other literature.
[10] T. Aushev *et al.* (Belle Collaboration), Phys. Rev. Lett. **93**, 201802 (2004).
[11] K. Vervink *et al.* (Belle Collaboration), Phys. Rev. D **80**, 111104 (2009).
[12] B. Aubert *et al.* (*BABAR* Collaboration), Phys. Rev. D **79**, 032002 (2009).
[13] R. Aleksan, I. Dunietz, B. Kayser, and F. Le Diberder, Nucl. Phys. **B361**, 141 (1991).
[14] B. Aubert *et al.* (*BABAR* Collaboration), Phys. Rev. Lett. **91**, 201802 (2003).
[15] S. Kurokawa and E. Kikutani, Nucl. Instrum. Methods Phys. Res., Sect. A **499**, 1 (2003), and other papers included in this volume.
[16] A. Abashian *et al.* (Belle Collaboration), Nucl. Instrum. Methods Phys. Res., Sect. A **479**, 117 (2002).
[17] K. F. Chen *et al.* (Belle Collaboration), Phys. Rev. D **72**, 012004 (2005).
[18] In this article the inclusion of charge conjugated decay modes is implied unless otherwise stated.
[19] M. Feindt and U. Kerzel, Nucl. Instrum. Methods Phys. Res., Sect. A **559**, 190 (2006).
[20] The Fox-Wolfram moments were introduced in G. C. Fox and S. Wolfram, Phys. Rev. Lett. **41**, 1581 (1978). The modified Fox-Wolfram moments used in this article are described in S. H. Lee *et al.* (Belle Collaboration), Phys. Rev. Lett. **91**, 261801 (2003).
[21] D. M. Asner *et al.* (CLEO Collaboration), Phys. Rev. D **53**, 1039 (1996).
[22] H. Albrecht *et al.* (ARGUS Collaboration), Phys. Lett. B **241**, 278 (1990).
[23] J. E. Gaiser *et al.* (Crystal Ball Collaboration), Phys. Rev. D **34**, 711 (1986).
[24] K. Nakamura *et al.* (Particle Data Group), J. Phys. G **37**, 075021 (2010).
[25] H. Kakuno *et al.*, Nucl. Instrum. Methods Phys. Res., Sect. A **533**, 516 (2004).
[26] H. Tajima *et al.*, Nucl. Instrum. Methods Phys. Res., Sect. A **533**, 370 (2004).
[27] O. Long, M. Baak, R. N. Cahn, and D. Kirkby, Phys. Rev. D **68**, 034010 (2003).
[28] K. Abe *et al.* (Belle Collaboration), Phys. Rev. Lett. **89**, 122001 (2002).